Enhanced electrocaloric and pyroelectric response from ferroelectric multilayers

M. T. Kesim, J. Zhang, S. P. Alpay, and L. W. Martin

Citation: Applied Physics Letters **105**, 052901 (2014); doi: 10.1063/1.4892455
View online: http://dx.doi.org/10.1063/1.4892455
View Table of Contents: http://scitation.aip.org/content/aip/journal/apl/105/5?ver=pdfcov
Published by the AIP Publishing

Articles you may be interested in

Influence of thermal stresses on the electrocaloric properties of ferroelectric films
Appl. Phys. Lett. **98**, 132907 (2011); 10.1063/1.3573788

Enhanced pyroelectric coefficient of antiferroelectric-ferroelectric bilayer thin films
J. Appl. Phys. **105**, 061610 (2009); 10.1063/1.3055350

Effective pyroelectric response of compositionally graded ferroelectric materials
Appl. Phys. Lett. **86**, 092903 (2005); 10.1063/1.1866505

Effect of operating temperature and film thickness on the pyroelectric response of ferroelectric materials
Appl. Phys. Lett. **84**, 4959 (2004); 10.1063/1.1762691

Pyroelectric response of ferroelectric thin films
J. Appl. Phys. **95**, 3618 (2004); 10.1063/1.1649460

AIP Chaos
CALL FOR APPLICANTS
Seeking new Editor-in-Chief

This article is copyrighted as indicated in the article. Reuse of AIP content is subject to the terms at: http://scitation.aip.org/termsconditions. Downloaded to IP: 128.32.121.33 On: Fri, 10 Oct 2014 18:29:05

Enhanced electrocaloric and pyroelectric response from ferroelectric multilayers

M. T. Kesim,[1] J. Zhang,[2] S. P. Alpay,[1,3,a)] and L. W. Martin[2,4]
[1]*Department of Materials Science and Engineering and Institute of Materials Science, University of Connecticut, Storrs, Connecticut 06269, USA*
[2]*Department of Materials Science and Engineering/Materials Research Laboratory, University of Illinois, Urbana–Champaign, Urbana, Illinois 61801, USA*
[3]*Department of Physics, University of Connecticut, Storrs, Connecticut 06269, USA*
[4]*Department of Materials Science and Engineering, University of California, Berkeley, California 94720, USA*

(Received 23 May 2014; accepted 26 July 2014; published online 4 August 2014)

Room temperature pyroelectric properties and adiabatic temperature change of (001)-textured ferroelectric multilayers on Si are computed by taking into account electrostatic interlayer interactions and thermal strains. We show that by adjusting internal electrical fields through changing relative thicknesses in a multilayer ferroelectric construct, electrothermal properties can be significantly enhanced. A quantitative analysis is provided for $BaTiO_3$-$PbZr_{0.2}Ti_{0.8}O_3$ (BTO-PZT) and $SrTiO_3$-$PbZr_{0.2}Ti_{0.8}O_3$ (STO-PZT) multilayers. For instance, $0.74 \times$ BTO-$0.26 \times$ PZT and $0.35 \times$ STO-$0.65 \times$ PZT bilayers show ~120% and 65% increase in electrocaloric response, respectively, compared to PZT films on Si for $\Delta E = 500$ kV/cm. © *2014 AIP Publishing LLC*. [http://dx.doi.org/10.1063/1.4892455]

The electrocaloric (EC) effect is the reversible adiabatic heating/cooling of a system by application/removal of an electric field. It is analogous to magnetocaloric and elastocaloric responses for which the external stimuli to induce a temperature change are magnetic and strain fields, respectively. All caloric properties of ferroic materials are attributed to a change in the entropy density through alignment of dipoles and/or structural alterations on the atomic, molecular, or microstructural level.[1–5] Electrocaloric materials (ECMs) have been investigated extensively as potential solid state cooling elements in devices with higher efficiency and offering more environmentally friendly refrigeration compared to existing vapor compression/expansion technology.[2] The EC response and its converse effect pyroelectricity are described by the same property coefficient, $p = (\partial S/\partial E)_T = (\partial P/\partial T)_E$ where S is entropy, T is temperature, E is the electric field, and P is the polarization. Materials displaying pyroelectricity can be employed in infrared (IR) devices for intrusion and fire detectors, uncooled thermal imagers, radiometers, and gas/laser analyzers.[6] A number of ECMs have been proposed for electrothermal applications, including, but not limited to, ferroelectric (FE) and anti-ferroelectric ceramics, polymers, and copolymers, in bulk, single crystal, and thin film forms.[1,2,4,7]

Early attempts to investigate the EC effect were made for ferroelectric bulk ceramics. The observed adiabatic temperature change ΔT of a couple of degrees is not sufficient for these materials to be utilized in device applications.[7–9] The major obstacle in obtaining high ΔTs from bulk materials is related to the magnitude of electric fields that can be applied and their relatively low dielectric breakdown strength. In 2006, the observation of $\Delta T \sim 12$ K at 776 kV/cm from a thin film FE propelled renewed interest in ECMs.[10] Since then, there have been many experimental[10–13] and theoretical[14–17] attempts to investigate the EC effect of thin films. ΔTs as high as 40 K have been reported at large fields exceeding the breakdown strength of bulk materials. Thin films not only permit high fields but also they can be integrated with microelectronic devices which is promising for the realization of on-chip EC micro-cooling systems.

Electrothermal response can be enhanced in the vicinity of a FE-paraelectric (PE) phase transition, especially if such a transition is of first order. It has been shown that the phase transition characteristics of FE films, and thus the accompanying electrothermal properties, could be influenced and tailored by thermal[18,19] and misfit strains,[20] lateral clamping of the film to the substrate,[20] domain structure,[17,21] film/substrate texture,[22] and thickness.[15] Another way to manipulate electrical properties of FEs is by constructing artificial multilayer heterostructures. FE/PE or FE/dielectric multilayers, superlattices, and compositionally graded stacks demonstrate peculiar electrical properties as compared to their bulk and single-crystal equivalents due to electrostatic and electromechanical interlayer interactions.[23,24] Such interactions not only alter the phase transition characteristics of individual layers but may also suppress spontaneous polarization entirely. Theoretical studies show that there exists a dielectric anomaly in coupled FE-PE bilayers at a critical PE layer fraction (α_C) associated with the disappearance of the ferroelectric response.[25] This phenomenon is similar to the dielectric maxima observed near T_C in monolithic FEs and can be used to enhance second-order property coefficients near α_C.[25] In fact, this idea has been utilized in the development of multilayer FEs with improved dielectric tunability for microwave telecommunication device applications.[26]

Lead zirconate titanate [$Pb(Zr_xTi_{1-x}O)_3$, (PZT x:$(1-x)$)] thin films with $x \leq 0.5$ exhibit relatively large electrothermal response at room temperature (RT = 25 °C).[27,28] These films can be deposited/grown via rf-sputtering, pulsed-laser

a)Author to whom correspondence should be addressed. Electronic mail: p.alpay@ims.uconn.edu

 © 2014 AIP Publishing LLC

This article is copyrighted as indicated in the article. Reuse of AIP content is subject to the terms at: http://scitation.aip.org/termsconditions. Downloaded to IP: 128.32.121.33 On: Fri, 10 Oct 2014 18:29:05

deposition, metal-organic chemical vapor deposition, and chemical solution deposition. The integration of PZT films into fully processed and metallized silicon (Si) as end-of-line processes is crucial for integrated circuit compatibility and cost considerations. However, the large coefficient of thermal expansion (CTE) mismatch between PZT and Si leads to formation of substantial thermal stresses that may affect the physical and electrical characteristics of such films. A summary of pyroelectric properties of PZT thin films on Si substrates is provided in Kesim *et al.* wherein it is shown that typical growth conditions yield pyroelectric coefficients of 0.02–0.04 $\mu C \times cm^{-2}\,^{\circ}C^{-1}$ for tetragonal PZT compositions at RT.[19]

One way of improving the pyroelectric and thus the EC properties for PZT films is through coupling PZT layers with other FE, PE, and dielectric materials, making use of the internal electric fields that are generated due to the polarization mismatch in a multilayer heterostructure configuration. In this study, we investigate the effect of interlayer coupling on electrothermal properties of [001]-textured polycrystalline PZT multilayers on Si as a function of relative PZT layer fraction. We employ here a thermodynamic model that takes into account formation of thermal stresses during cooling from the growth/processing temperature (T_G) and the electrostatic coupling between individual layers. Schematics of heterostructures analyzed theoretically are shown in Fig. 1. Specifically, we concentrate on PZT-$BaTiO_3$ (BTO) and PZT-$SrTiO_3$ (STO) multilayers as examples corresponding to different strengths of electrostatic coupling. We also note that the loss and leakage characteristics of barium strontium titanate films in electrically tunable device applications can be improved by employing STO buffer layers.[26] As such, it is important to describe electrothermal properties of PZT-STO multilayers in the configuration shown in Fig. 1(b), since such a construct would have an added benefit of limiting charge injection from the electrodes and hence reducing leakage currents.

Schematic representations of the multilayers investigated here are shown in Fig. 1. The films are considered to be poled along [001] such that they are in a monodomain state. The out-of-plane caloric responses were then computed from relevant thermodynamic relations. We assume that the multilayers are processed at $T_G = 600\,^{\circ}C$ before cooling to

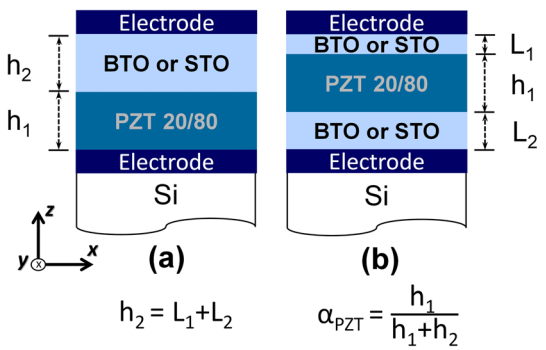

FIG. 1. Schematics of the two multilayer ferroelectric heterostructures analyzed theoretically: (a) BTO- and STO-PZT 20/80 bilayers and (b) trilayer BTO- and STO-PZT 20/80. In both cases the multilayer constructs are on relatively thick Si substrates and are sandwiched between top and bottom metallic electrodes.

RT. The in-plane strains $u_{T,i}$ between layer i and Si that develop during cooling from T_G to RT are given by

$$u_{T,i}(T_G) = \int_{T}^{T_G} (\alpha_{F,i} - \alpha_S) dT, \tag{1}$$

where $\alpha_{F,i}$ and α_S are the in-plane CTEs of layer i and the substrate, respectively. The substrate is assumed to be much thicker than the multilayer such that the thermal stresses are confined in the film. The total free energy density of such a system can be expressed as

$$G = (1-\alpha)\cdot G_1(P_1, T, u_{T,1}, E) + \alpha \cdot G_2(P_2, T, u_{T,2}, E) + \frac{1}{2}\alpha(1-\alpha)\frac{1}{\varepsilon_0}(P_1 - P_2)^2. \tag{2}$$

The details of the derivation of the above relation are given elsewhere.[25] Here, $\alpha = \alpha_{PZT} = h_2/(h_1 + h_2)$ is the relative thickness (layer fraction) of the PZT layer where h_1 and h_2 are the thicknesses of BTO or STO and PZT layers, respectively, and $h = h_1 + h_2$ is the total thickness of the multilayer. In Eq. (2), P_i is the polarization of layer i normal to the interlayer interface, and E is an applied electrical field parallel to the polarization direction. The last term in the above free energy functional expresses the electrostatic coupling between the layers. G_1 and G_2 are the uncoupled free energies of the FE and STO layers, respectively, given by

$$G_i(P_i, T, u_{T,i}, E) = G_{0,i} + \tilde{a}_i P_i^2 + \tilde{b}_i P_i^4 + c_i P_i^6 + \frac{u_{T,i}^2}{S_{11} + S_{12}} - E P_i, \tag{3}$$

with renormalized dielectric coefficients $\tilde{a}_i$ and $\tilde{b}_i$ for the clamped and strained case

$$\tilde{a}_i = a_i - \frac{2Q_{12,i}}{S_{11,i} + S_{12,i}} u_{T,i}, \quad \tilde{b}_i = b_i + \frac{Q_{12,i}^2}{S_{11,i} + S_{12,i}}, \tag{4}$$

where a_i, b_i, and c_i are the bulk dielectric stiffness coefficients. The quadratic coefficient a_i is given by the Curie-Weiss Law, $a_i = (T\text{-}T_{C,i})/2\varepsilon_0 C_i$, where ε_0 is the permittivity of free space and C_i are the Curie-Weiss constants. $Q_{ij,i}$ and $S_{ij,i}$ are the electrostrictive coefficients and the elastic compliances at constant polarization of layer i. We note that the free energy functional of the multilayer expressed through Eq. (2) is identical for the two configurations depicted in Fig. 1 if the layer thicknesses are much larger than the correlation length of ferroelectricity (of the order of 1–10 nm).[25] For the numerical analysis presented in this study, values for the coefficients entering Eqs. (2)–(4) were obtained from available literature.[16,29,30]

The equilibrium polarizations P_i^0 along the z-direction in the multilayer follow from the equations of state $\partial G/\partial P_i = 0$ and the average out-of-plane polarization of the multilayers is $= (1-\alpha)P_1^0 + \alpha P_2^0$. The pyroelectric coefficient and the adiabatic temperature change are given by

$$p(T,E) = \frac{d\langle P\rangle}{dT} = \frac{d\langle P_S\rangle}{dT} + \int_0^E \left(\frac{\partial\langle\varepsilon\rangle}{\partial T}\right)_E dE, \tag{5}$$

This article is copyrighted as indicated in the article. Reuse of AIP content is subject to the terms at: http://scitation.aip.org/termsconditions. Downloaded to IP: 128.32.121.33 On: Fri, 10 Oct 2014 18:29:05

$$\Delta T(T,E,u_T) = -\int_{E_a}^{E_b} \frac{T}{C_E(T,E,u_T)} \left(\frac{\partial \langle P(T,E,u_T)\rangle}{\partial T}\right)_E dE. \quad (6)$$

Here, $C_E(T, E, u_T)$ is the total heat capacity of the multilayer consisting of the excess heat capacity $C_E^{XS} = -T(\partial^2 G/\partial T^2)$ and lattice contributions fitted from experimental data.[31] We note that in order to improve the time response of pyroelectric elements, the high thermal conductivity Si substrate is usually back-etched at the end of device fabrication.[27,32,33] The thermal strains that are defined through Eq. (1) would still exist in FE film(s) and alter the equilibrium properties unless the pyroelectric elements are subjected to an annealing processing step. The same arguments may also hold for electrocaloric micro refrigeration systems. However, design parameters are quite different for such applications compared to a pyroelectric sensor and device fabrication may not require Si etching at all.[4,34–36]

The average out-of-plane polarizations and pyroelectric coefficients of BTO-PZT and STO-PZT multilayers on Si at RT are plotted in Fig. 2. T_C of BTO monolayer films ($\alpha_{PZT} = 0$) for $T_G = 600\,^\circ$C on Si is $-101\,^\circ$C, which is 219 °C lower than the stress-free bulk value of 120 °C. The shift of T_C to lower temperatures is related to in-plane tensile strains that develop during cooling from T_G to RT. Such variations in T_C due to tensile strains have been observed experimentally in polycrystalline FE films.[37–40] Therefore, BTO is in a PE state for $T_G = 600\,^\circ$C as indicated in Fig. 2(a) for $\alpha_{PZT} = 0$. With increasing fraction of PZT in the multilayer construct, electrostatic interactions become sufficiently large to induce FE in both layers. This occurs at a critical PZT layer fraction α_C such that for $\alpha_{PZT} > \alpha_C$, the heterostructure has a non-zero spontaneous polarization, $\langle P_S \rangle$. On the other hand, the polarization profiles of multilayers made up of STO and PZT look slightly different [Fig. 2(c)]. A higher critical PZT layer fraction ($\alpha_C = 0.65$) is required for STO-PZT multilayers compared to BTO-PZT, since electrostatic coupling between PZT and STO is weaker. This is because the induced polarization in STO from the internal electrostatic field is smaller due to the relatively smaller dielectric constant of STO compared to BTO. The relative small signal dielectric constants of STO and BTO for thermal strains corresponding to $T_G = 600\,^\circ$C on Si are 241 and 1270, respectively; hence, STO-PZT multilayers in the FE state vanishes at a much higher α_{PZT} than BTO-PZT multilayers. In order to obtain a substantial total polarization from STO-PZT heterostructures, PZT-rich multilayer constructs ($0.65 < \alpha_{PZT} < 1$) should be preferred. Electrostatic interactions also change the phase transition characteristics of the heterostructures by altering T_C of the layers; this is consistent with the discussion above.[41]

The pyroelectric coefficient defined via Eq. (5) has two components. The first term is the change in the spontaneous polarization in the FE phase and the second term corresponds to the temperature variation of the induced polarization which only becomes significant in the PE phase where $P_S = 0$. The former is usually preferred in applications for intrusion detectors and gas analyzers where the pyroelectric elements become active upon external electric field stimuli. On the contrary, the PE state requires a bias field to obtain an induced pyroelectric response that could be used in IR imaging arrays due higher dielectric constant values near T_C. Electric field dependent RT pyroelectric coefficients of BTO-PZT and STO-PZT multilayers on Si as a function of PZT layer fraction are plotted in Figs. 2(b) and 2(d), respectively. Zero field pyroelectric coefficient of both multilayers exhibits a jump near α_C. The pyroelectric coefficients of BTO-PZT and STO-PZT multilayers are $\sim 0.45\,\mu$C $\times$ cm^{-2} °C^{-1} at $\alpha_{PZT} = 0.26$ and $\alpha_{PZT} = 0.65$, respectively. This value, which is an order of magnitude larger than the pyroelectric response of PZT monolayers on Si ($p_{PZT} = 0.041\,\mu$C $\times$ cm^{-2} °C^{-1}), clearly indicates a marked

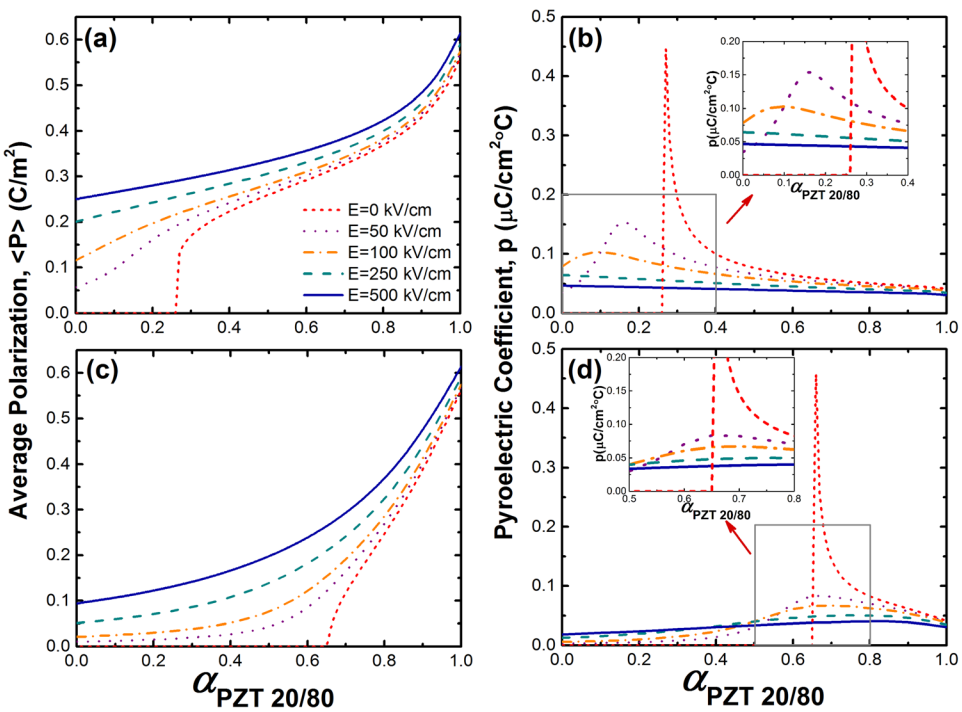

FIG. 2. (a) and (c) Display the average RT polarization of BTO-PZT 20/80 and STO-PZT 20/80 heterostructures as a function of α_{PZT} and its dependence on applied electric field parallel to the polarization (z-) direction. (b) and (d) The total RT pyroelectric coefficient of heterostructures with polarizations given in (a) and (c). T_G was taken to be 600 °C in these calculations. The insets to (b) and (d) illustrate the pyroelectric response in the vicinity of the polarization anomaly. There is a significant enhancement of the pyroelectric coefficient over monolithic PZT.

This article is copyrighted as indicated in the article. Reuse of AIP content is subject to the terms at: http://scitation.aip.org/termsconditions. Downloaded to IP: 128.32.121.33 On: Fri, 10 Oct 2014 18:29:05

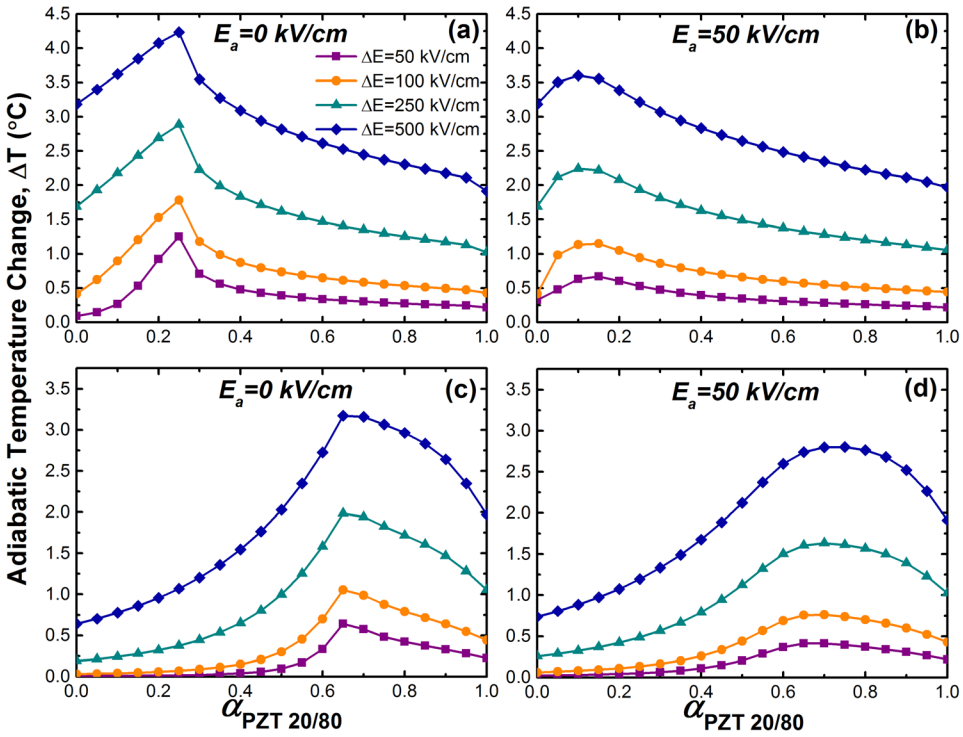

FIG. 3. RT adiabatic temperature changes of BTO-PZT 20/80 and STO-PZT 20/80 heterostructures at $E_a = 0$ kV/cm as a function of α_{PZT} and driving field, ΔE are shown in (a) and (c), respectively. ΔT of same heterostructures at $E_a = 50$ kV/cm are also plotted in (b) and (d) for comparison.

improvement in the pyroelectric properties. When multilayers are in a PE state, i.e., $\alpha_{PZT} < \alpha_C$, a pyroelectric response can only be realized under bias. For example, the pyroelectric coefficient of $0.84 \times$ BTO-$0.16 \times$ PZT multilayers under 50 kV/cm bias is 0.15 μC/cm^2 °C, see inset in Fig. 2(b). This value is significantly larger than the pyroelectric response of monolithic BTO and PZT on Si (at 50 kV/cm, $p_{\mathrm{BTO}} = 0.035\ \mu\mathrm{C} \times \mathrm{cm}^{-2}\ ^\circ\mathrm{C}^{-1}$ and $p_{\mathrm{PZT}} = 0.038\ \mu\mathrm{C} \times \mathrm{cm}^{-2}\ ^\circ\mathrm{C}^{-1}$). Another interesting feature for BTO-PZT multilayers is that the anomaly at α_C is shifted to lower numbers with a broadened pyroelectric response under moderate fields (0–100 kV/cm). These calculations suggest that if the pyroelectric detector is designed to work in the bolometer mode, the layer fraction of PZT can be adjusted for a specific operating field in the low field regime (0–100 kV/cm) to optimize pyroelectric properties.

The RT adiabatic temperature change for BTO-PZT and STO-PZT is plotted in Fig. 3 as a function of initial bias field E_a, electric field difference $\Delta E = E_{final} - E_a$, and α_{PZT}. EC effect is more pronounced at higher ΔE as expected, since dipoles are aligned more readily at stronger fields leading to a higher excess entropy density change. As an example, ΔT of $0.35 \times$ STO-$0.65 \times$ PZT for $E_a = 0$ kV/cm is increased almost six times from 0.63 °C to 3.17 °C with $\Delta E = 500$ kV/cm. Although the EC response near the dielectric anomaly slightly deteriorates with an initial bias [($E_a = 50$ kV/cm, Figs. 3(b) and 3(d)], it becomes less sensitive to α_{PZT}. Moreover, the peak at α_C is shifted to lower and higher PZT layer fractions for field-driven BTO-PZT and STO-PZT multilayers, respectively, compared to zero field EC response. This effect can be explained through the polarization profiles of the multilayers as the electrostatically induced phase transition is smeared upon the application of applied electric fields [Figs. 2(a) and 2(c)]. Fig. 3 shows clearly that it is possible to significantly enhance the RT EC properties of PZT by constructing multilayer FE heterostructures. For instance, $0.74 \times$ BTO-$0.26 \times$ PZT and $0.35 \times$ STO-$0.65 \times$ PZT bilayers show ~120% and 65% increase in the electrocaloric response, respectively, compared to PZT films on Si for $\Delta E = 500$ kV/cm and $E_a = 50$ kV/cm.

In summary, RT electrothermal properties of PZT-based multilayers on Si can be tailored depending on the choice of the mating layer and the PZT layer fraction. The key observation of this work is how the multilayer structure/geometry, in particular the role of electrostatic interactions between the FE and PE layers, can influence the phase transition characteristics driving enhanced thermal and electrical susceptibility of the composite structure. Based on this insight, we suggest that the BTO-PZT system may be a good candidate material for IR applications, since the multilayers can operate with or without a bias depending on α_{PZT} with large pyroelectric coefficients. On the other hand, although the overall EC response of BTO-PZT multilayers is higher than STO-PZT, heterostructures with STO layers would further improve the loss and leakage characteristics of such films with significant enhancement in ΔT relative to PZT monolayers.

J. Z. acknowledges the support from the Army Research Office under grant W911NF-10-1-0482 and the Air Force Office of Scientific Research under Grant FA9550-11-1-0073. L.W.M. acknowledges the support from the National Science Foundation under Grant DMR-1149062.

[1]J. F. Scott, Annu. Rev. Mater. Res. **41**, 229 (2011).
[2]M. Valant, Prog. Mater. Sci. **57**, 980 (2012).
[3]M. M. Vopson, J. Phys. D: Appl. Phys. **46**, 345304 (2013).
[4]M. Ožbolt, A. Kitanovski, J. Tušek, and A. Poredoš, Int. J. Refrig. **40**, 174 (2014).
[5]K. A. Gschneidner and V. K. Pecharsky, Int. J. Refrig. **31**, 945 (2008).
[6]R. W. Whatmore, J. Electroceram. **13**, 139 (2004).
[7]S.-G. Lu and Q. Zhang, Adv. Mater. **21**, 1983 (2009).

This article is copyrighted as indicated in the article. Reuse of AIP content is subject to the terms at: http://scitation.aip.org/termsconditions. Downloaded to IP: 128.32.121.33 On: Fri, 10 Oct 2014 18:29:05

[8]M. Valant, A.-K. Axelsson, F. Le Goupil, and N. M. Alford, Mater. Chem. Phys. **136**, 277 (2012).
[9]B. A. Tuttle and D. A. Payne, Ferroelectrics **37**, 603 (1981).
[10]A. Mischenko, Q. Zhang, J. F. Scott, R. W. Whatmore, and N. D. Mathur, Science **311**, 1270 (2006).
[11]R. Chukka, J. W. Cheah, Z. Chen, P. Yang, S. Shannigrahi, J. Wang, and L. Chen, Appl. Phys. Lett. **98**, 242902 (2011).
[12]X. Hao, Z. Yue, J. Xu, S. An, and C.-W. Nan, J. Appl. Phys. **110**, 064109 (2011).
[13]S. G. Lu, B. Rožič, Q. M. Zhang, Z. Kutnjak, X. Li, E. Furman, L. J. Gorny, M. Lin, B. Malič, M. Kosec, R. Blinc, and R. Pirc, Appl. Phys. Lett. **97**, 162904 (2010).
[14]B. Li, J. B. Wang, X. L. Zhong, F. Wang, and Y. C. Zhou, J. Appl. Phys. **107**, 014109 (2010).
[15]J. H. Qiu and Q. Jiang, J. Appl. Phys. **103**, 084105 (2008).
[16]J. Zhang, A. A. Heitmann, S. P. Alpay, and G. A. Rossetti, J. Mater. Sci. **44**, 5263 (2009).
[17]J. Karthik and L. W. Martin, Appl. Phys. Lett. **99**, 032904 (2011).
[18]S. H. Oh and H. M. Jang, Appl. Phys. Lett. **72**, 1457 (1998).
[19]M. T. Kesim, J. Zhang, S. Trolier-McKinstry, J. V. Mantese, R. W. Whatmore, and S. P. Alpay, J. Appl. Phys. **114**, 204101 (2013).
[20]G. Akcay, S. P. Alpay, G. A. Rossetti, and J. F. Scott, J. Appl. Phys. **103**, 024104 (2008).
[21]J. Karthik, J. C. Agar, A. R. Damodaran, and L. W. Martin, Phys. Rev. Lett. **109**, 257602 (2012).
[22]H.-X. Cao, V. C. Lo, and Z.-Y. Li, J. Appl. Phys. **101**, 014113 (2007).
[23]M. B. Okatan, J. V. Mantese, and S. P. Alpay, Acta Mater. **58**, 39 (2010).
[24]R. V. K. Mangalam, J. C. Agar, A. R. Damodaran, J. Karthik, and L. W. Martin, ACS Appl. Mater. Interfaces **5**, 13235 (2013).
[25]A. L. Roytburd, S. Zhong, and S. P. Alpay, Appl. Phys. Lett. **87**, 092902 (2005).
[26]M. W. Cole, E. Ngo, C. Hubbard, S. G. Hirsch, M. Ivill, W. L. Sarney, J. Zhang, and S. P. Alpay, J. Appl. Phys. **114**, 164107 (2013).
[27]P. Muralt, J. Micromech. Microeng. **10**, 136 (2000).
[28]R. Bruchhaus, D. Pitzer, R. Primig, M. Schreiter, W. Wersing, N. Neumann, N. Hess, J. Vollheim, R. Kohler, and M. Simon, Integr. Ferroelectr. **17**, 369 (1997).
[29]M. J. Haun, Z. Q. Zhuang, E. Furman, S. J. Jang, and L. E. Cross, Ferroelectrics **99**, 45 (1989).
[30]N. A. Pertsev, A. G. Zembilgotov, and A. K. Tagantsev, Phys. Rev. Lett. **80**, 1988 (1998).
[31]F. Jona and G. Shirane, *Ferroelectric Crystals* (Dover, New York, 1962), p. 124.
[32]W. Liu, J. S. Ko, and W. Zhu, Thin Solid Films **371**, 254 (2000).
[33]B. Willing, M. Kohli, P. Muralt, and O. Oehler, Infrared Phys. Techtol. **39**, 443 (1998).
[34]M. Ožbolt, A. Kitanovski, J. Tušek, and A. Poredoš, Int. J. Refrig. **37**, 16 (2014).
[35]D. Guo, J. Gao, Y.-J. Yu, S. Santhanam, A. Slippey, G. K. Fedder, A. J. H. McGaughey, and S.-C. Yao, Int. J. Heat Mass Transfer. **72**, 559 (2014).
[36]Y. S. Ju, J. Electron. Packag. **132**, 041004 (2010).
[37]T. R. Taylor, P. J. Hansen, B. Acikel, N. Pervez, R. A. York, S. K. Streiffer, and J. S. Speck, Appl. Phys. Lett. **80**, 1978 (2002).
[38]D. A. Tenne, A. Soukiassian, X. X. Xi, T. R. Taylor, P. J. Hansen, J. S. Speck, and R. A. York, Appl. Phys. Lett. **85**, 4124 (2004).
[39]M. T. Kesim, M. W. Cole, J. Zhang, I. B. Misirlioglu, and S. P. Alpay, Appl. Phys. Lett. **104**, 022901 (2014).
[40]S. Song, J. Zhai, L. Gao, and X. Yao, Appl. Phys. Lett. **94**, 052902 (2009).
[41]A. P. Levanyuk and I. B. Misirlioglu, J. Appl. Phys. **110**, 114109 (2011).

This article is copyrighted as indicated in the article. Reuse of AIP content is subject to the terms at: http://scitation.aip.org/termsconditions. Downloaded to IP: 128.32.121.33 On: Fri, 10 Oct 2014 18:29:05